Increasing the Affinity of a Human IgG1 for the Neonatal Fc Receptor: Biological Consequences[1]

William F. Dall' Acqua,[2]* Robert M. Woods,* E. Sally Ward,† Susan R. Palaszynski,* Nita K. Patel,* Yambasu A. Brewah,* Herren Wu,* Peter A. Kiener,* and Solomon Langermann*

Many biological functions, including control of the homeostasis and maternofetal transfer of serum γ-globulins, are mediated by the MHC class I-related neonatal FcR (FcRn). A correlation exists in mice between the binding affinity of IgG1/Fc fragments to FcRn at pH 6.0 and their serum $t_{1/2}$. To expand this observation, phage display of mutagenized Fc fragments derived from a human IgG1 was used to increase their affinity to both murine and human FcRn. Ten variants were identified that have a higher affinity toward murine and human FcRn at pH 6.0, with ΔΔG ($\Delta G_{wild\ type} - \Delta G_{mutant}$) from 1.0 to 2.0 kcal/mol and from 0.6 to 2.4 kcal/mol, respectively. Those variants exhibit a parallel increase in binding at pH 7.4 to murine, but not human, FcRn. Although not degraded in blood in vitro, accumulated in tissues, nor excreted in urine, their serum concentration in mice is decreased. We propose that higher affinity to FcRn at pH 7.4 adversely affects release into the serum and offsets the benefit of the enhanced binding at pH 6.0. ***The Journal of Immunology*****, 2002, 169: 5171–5180.**

The protection of IgGs from degradation as well as the maternofetal transfer of IgG from mother to young are essential, tightly controlled processes in mammals. The neonatal FcR (FcRn)[3] plays a central role in both of these events (1). Much is known about the role of FcRn in rodents, in which it has been shown to mediate transcytosis of IgGs across the epithelium of the neonatal intestine (2), yolk sac (3), and mammary gland (4), as well as to maintain constant levels of serum IgG (5, 6). In humans, FcRn is also believed to play a role in IgG transport. This has been shown both for placenta (7, 8) and adult epithelia (9, 10). A role for FcRn in IgG homeostasis in humans has been hypothesized (5, 11, 12), but to date, there is no direct evidence to invoke its role in such a process.

FcRn is a heterodimer formed by the association of an L (β_2-microglobulin) and H (α-chain) (13) chain. The α-chain, composed of three domains (α1, α2, and α3), is anchored to the membrane via a transmembrane region. The rat, murine, and human H chain sequences (7, 13, 14) as well as the rat and human FcRn structures (15–17) are homologous to the class I major histocompatibility complex molecules. Crystallographic studies of the extracellular domain of unliganded human FcRn (17) and of the extracellular domain of rat FcRn free and bound to rat IgG (15, 16) have indicated that human and rat FcRn are structurally similar. The most notable feature of the interaction of murine and human FcRn with murine and human IgG is its pH dependency: the Fc portion of IgGs binds FcRn with a high affinity at pH 6.0 and is released at pH 7.2 (2, 18). This suggests, along with colocalization studies (19), that for cells bathed in near neutral pH, the IgG/FcRn complex forms within acidified endosomes. More precisely, FcRn acts as a salvage receptor, binding and transporting pinocytosed IgGs in intact form both within and across cells, and rescuing them from a default degradative pathway. Although the molecular mechanisms responsible for salvaging IgGs are still largely unknown, it is thought that unbound IgGs are directed toward proteolysis in lysosomes, whereas bound Igs are recycled to the surface of the cells and released. This control takes place within the endothelial cells located diffusely throughout adult tissues (5, 20).

Fc residues critical to the mouse Fc-mouse FcRn interaction have been identified by site-directed mutagenesis. In particular, I253, H310, H433, N434, and H435 (EU numbering) (21) are major components of the functional epitope (3, 8, 22) in which H310 and H435 are responsible for the pH dependence of binding (23). I253, H310, and H435 were found to be critical for the interaction of human Fc with murine FcRn (12). Likewise, studies of the human Fc-human FcRn complex have demonstrated the crucial role played by I253, S254, H435, and Y436 (8, 24). Functional epitopes on the rat FcRn have been also identified by site-directed mutagenesis in both the α-chain and β_2-microglobulin chain (25, 26), demonstrating which residues on the FcRn are critical for the interaction with both mouse and rat IgG.

There seems to be a correlation between decrease (3) and increase (11) in the affinity of murine hinge-Fc fragments for murine FcRn at pH 6.0 and their serum $t_{1/2}$ in mice. The same correlation exists when one considers the interaction of human hinge-Fc fragments with mouse FcRn (8, 12). This observation has obvious relevance for the generation of therapeutic Abs with increased serum persistence. Although it has been proposed that a tighter IgG-FcRn interaction at pH 7.5 can result in a decreased IgG serum persistence (27), this phenomenon has not been investigated in detail. Furthermore, most of the studies published to date have been limited to the analysis of the interaction of rodent FcRn with rodent or human IgGs (3, 11, 12, 16, 22, 23, 26, 28–30). Recent studies involving the binding of human IgGs to human FcRn have

*MedImmune, Gaithersburg, MD 20878; and †Center for Immunology and Cancer Immunobiology Center, University of Texas Southwestern Medical Center, Dallas, TX 75390

Received for publication June 25, 2002. Accepted for publication September 3, 2002.

The costs of publication of this article were defrayed in part by the payment of page charges. This article must therefore be hereby marked *advertisement* in accordance with 18 U.S.C. Section 1734 solely to indicate this fact.

[1] This work was supported in part by a grant from the National Institutes of Health to E.S.W. (AI RO1 39167).

[2] Address correspondence and reprint requests to Dr. William F. Dall'Acqua, Department of Protein Engineering, MedImmune, Inc., 35 West Watkins Mill Road, Gaithersburg, MD 20878. E-mail address: dall'acquaw@medimmune.com

[3] Abbreviations used in this paper: FcRn, neonatal FcR; RU, resonance unit; SPR, surface plasmon resonance.

0022-1767/02/$02.00

provided important information, such as the role of the receptor in the maternofetal transfer of γ-globulin (8), the chemical nature of the interface, and general characteristics of the interaction (17), as well as the relative contribution of individual residues to the energetics of complex formation (24). Human Fc mutants with all solvent-exposed residues along the C_H2 and C_H3 domains substituted by alanine were produced (24). This led to the identification of >12 variants with increased affinity to the human receptor, most by a factor of 1.5- to 2-fold. Two combination mutants showed increased affinity by up to 12-fold (24).

We have now further characterized the human Fc-human FcRn and human Fc-mouse FcRn interactions. Using rationally designed libraries and phage display, we provide evidence that a human IgG1 can be engineered for large (>30 times) increases in affinity toward both human and murine FcRn. As a step toward a better understanding of these interactions, we investigated the binding of different IgG1 variants at neutral pH. We show that IgG1 mutants exhibiting an increase in affinity toward murine FcRn by a factor of >5-fold at pH 6.0 also show significantly better binding at pH 7.4 when compared with the wild-type molecule. In contrast, IgG1 mutants exhibiting an affinity increase toward human FcRn by a factor of up to 10-fold at pH 6.0 all bind very poorly at pH 7.4. When injected in equal amounts into different BALB/c mice, three IgG1 variants with a 1.4- to 19-fold affinity increase to murine FcRn at pH 6.0 exhibit lower than wild-type serum concentrations (reported in $ng_{variant/wild\ type}/ml_{serum}$). Those mutants are not proteolyzed more efficiently than a wild-type control in serum or whole blood, nor are they seen to accumulate in different tissues or be excreted at a detectable level in urine. We hypothesize that retention of binding at neutral pH offsets the advantage of improved binding at pH 6.0, leading to the intracellular sequestration of the corresponding IgG molecules in FcRn-containing tissues.

Our results suggest that the pH dependency of binding of IgG1 to FcRn plays a critical role in determining the biological effect of an affinity-improving substitution.

Materials and Methods

Reagents

All chemicals were of analytical grade. Restriction enzymes and DNA-modifying enzymes were purchased from New England Biolabs (Beverly, MA). TG1 and CJ236 *Escherichia coli* were obtained from APBiotech (Piscataway, NJ) and Bio-Rad (Richmond, CA), respectively.

Expression and purification of murine and human FcRn

Recombinant mouse and human FcRn were produced as described (8, 29). Human FcRn was also obtained following isolation from human placenta cDNA (Clontech, Palo Alto, CA) of the genes for human β_2-microglobulin (21) and codons −23–267 of the human α-chain (7) using standard PCR protocols. L and H chains along with their native signal sequence (7, 21) were cloned in pFastBac DUAL and pFastBac1 bacmids, respectively, and viral stocks produced in *Spodoptera frugiperda* cells (Sf9) according to the manufacturer's instructions (Invitrogen, Carlsbad, CA). High-Five cells were infected at a multiplicity of infection of 3 with the baculoviruses encoding α- and β_2-chains using commercially available protocols (Invitrogen). Supernatant of infected insect cells was then adjusted to pH 6.0 with hydrochloric acid and applied to a 10 ml IgG Sepharose 6 Fast Flow column (APBiotech). The resin was washed with 200 ml 50 mM MES, pH 6.0, and FcRn eluted with 0.1 M Tris-Cl, pH 8.0. Purified FcRn (>95% homogeneity, as judged by SDS-PAGE) was dialyzed against PBS, flash frozen, and stored at −70°C.

Construction of IgG1/Fc libraries

A human hinge-Fc gene spanning aa residues 226–478 (Kabat numbering) (21), derived from MEDI-493 human IgG1 (31), was cloned into the pCANTAB5E phagemid vector (APBiotech) as an *Sfi*I/*Not*I fragment. Four libraries were generated by introducing random mutations at positions 251, 252, 254, 255, 256 (library 1); 308, 309, 311, 312, 314 (library 2); 385, 386, 387, 389 (library 3); and 428, 433, 434, 436 (library 4), using a Kunkel-based strategy (32). Briefly, four distinct hinge-Fc templates were generated using PCR by overlap extension (33), each containing one TAA stop codon at position 252 (library 1), 310 (library 2), 384 (library 3), or 429 (library 4), so that only mutagenized phagemids will give rise to Fc-displaying phage. Each TAA-containing ssDNA (TAAssDNA) was then prepared as follows: a single CJ236 *E. coli* colony harboring one of the four relevant TAA-containing phagemid was grown in 10 ml 2× YT medium supplemented with 10 μg/ml chloramphenicol and 100 μg/ml ampicillin. At OD_{600} = 1, VCSM13 helper phage (Stratagene, La Jolla, CA) was added to a final concentration of 10^{10} PFU/ml. After 2 h, the culture was transferred to 500 ml of 2× YT medium supplemented with 0.25 μg/ml uridine, 10 μg/ml chloramphenicol, 30 μg/ml kanamycin, and 100 μg/ml ampicillin, and grown overnight at 37°C. Phage were precipitated with PEG6000 using standard protocols (34) and purified using the Qiaprep Spin M13 Kit (Qiagen, Valencia, CA), according to the manufacturer's instructions. A total of 10–30 μg of each uracil-containg TAAssDNA template was then combined with 0.6 μg of the following phosphorylated oligonucleotides (MWG Biotech, High Point, NC) in 50 mM Tris-HCl, 10 mM $MgCl_2$, pH 7.5, in a final volume of 250 μl (randomized regions are underlined): library 1, 5′-CATGTGACCTCAGGSNNSNNSNNGATSNNSNNGGTGTCCTTGGGTTTTGGGGGG-3′; library 2, 5′-GCACTTGTACTCCTTGCCATTSNNCCASNNSNNGTGSNNSNNGGTGAGGACGC-3′; library 3, 5′-GGTCTTGTAGTTSNNCTCSNNSNNSNNATTGCTCTCCC-3′; library 4, 5′-GGCTCTTCTGCGTSNNGTGSNNSNNCAGAGCCTCATGSNNCACGGAGCATGAG-3′.

Each mixture was incubated at 90°C for 2 min, 50°C for 3 min, and 20°C for 5 min. Synthesis of the heteroduplex DNA was conducted by adding 30 U of both T4 DNA ligase and T7 DNA polymerase in presence of 0.4 mM ATP, 1 mM dNTPs, and 6 mM DTT. The mixture was incubated for 4 h at 20°C. Heteroduplex DNA was affinity purified and desalted using the Qiaquick DNA purification kit (Qiagen). A total of 1–5 μg of heteroduplex DNA was then electroporated into 300 μl of electrocompetent TG1 *E. coli* cells in a 2.5 kV field using 200 Ω resistance and 25 μF capacitance until a library size of 1×10^8 (library 1 and 2) or 1×10^7 (library 3 and 4) was reached. Cells were grown in 500 ml of 2× YT medium containing 100 μg/ml ampicillin and 10^{10} PFU/ml of VCSM13 helper phage overnight at 37°C. Phage were precipitated with PEG6000, as previously described (34).

Selection of the Fc libraries

Phage were resuspended in 5 ml 20 mM MES, pH 6.0/5% skimmed milk/0.05% Tween 20 and added (100 μl of 5×10^{12} PFU/ml/well) to 20 wells of a Maxisorp immunoplate (Nunc, Rochester, NY) previously coated with 1 μg of murine FcRn and blocked with 5% skimmed milk. After incubation for 2 h at 37°C, wells were washed 10–30 times with 20 mM MES, pH 6.0/0.2% Tween 20/0.3 M NaCl and phage eluted by incubation in 100 μl PBS, pH 7.4/well for 30 min at 37°C. Phage were used to reinfect exponentially growing *E. coli* TG1, as described (35). Three to six rounds of panning were conducted. Typically, 20–40 clones were characterized after three (library 1, 2, and 4) and six (library 3) rounds of panning by dideoxynucleotide sequencing (36) using a ABI3000 genomic analyzer (Applied Biosystems, Foster City, CA).

Construction, production, and purification of IgG1 variants

Representative Fc mutations were incorporated into the human IgG1 MEDI-493 (31). The H chain was subjected to site-directed mutagenesis using a Quick Change Mutagenesis kit (Stratagene), according to the manufacturer's instructions, and sequences were verified using a ABI3000 sequencer. The different constructs were expressed transiently in human embryonic kidney 293 cells using a CMV immediate-early promoter and dicistronic operon in which the γ1 chain is cosecreted with the κ-chain (31). IgG1s were purified from the conditioned medium directly on 1 ml HiTrap protein A columns, according to the manufacturer's instructions (APBiotech).

Surface plasmon resonance (SPR) measurements

The interaction of soluble murine and human FcRn with immobilized human IgG1 variants was monitored by SPR detection using a BIAcore 3000 instrument (Pharmacia Biosensor, Uppsala, Sweden). No aggregated FcRn that could interfere with affinity measurements (37, 38) was detected by gel filtration. Protein concentrations were calculated by the bicinchoninic acid method for both human and murine FcRn or using the 1% extinction coefficient at 280 nm of 1.5 for IgG1 wild type and variants. IgGs were coupled to the dextran matrix of a CM5 sensor chip (Pharmacia Biosensor) using an amine coupling kit, as described (39). The protein concentrations ranged from 3 to 5 μg/ml in 10 mM sodium acetate, pH 5.0. The activation period was set for 7 min at a flow rate of 10 μl/min, and the immobilization

period was set to between 10 and 20 min at a flow rate of 10 μl/min. Excess reactive esters were quenched by injection of 70 μl of 1.0 M ethanolamine hydrochloride, pH 8.5. This typically resulted in the immobilization of between 500 and 4000 resonance units (RU). Human and murine FcRn were buffer exchanged against 50 mM PBS, pH 6.0, 7.4, or 8.5, containing 0.05% Tween 20. Dilutions were made in the same buffers. All binding experiments were performed at 25°C, with concentrations ranging from 2.86 μM to 1 nM at a flow rate of 5–10 μl/min; data were collected for 25–50 min, and three 1-min pulses of PBS, pH 7.4, were used to regenerate the surfaces. FcRn was also flowed over an uncoated cell, and the sensorgrams from these blank runs were subtracted from those obtained with IgG1-coupled chips. Runs were analyzed using the software BIAevaluation 3.1 (Pharmacia Biosensor). Association constants (K_a) were determined from Scatchard analysis by measuring the concentration of free reactants and complex at equilibrium after correction for nonspecific binding (40). Errors were estimated as the SD for two or three independent determinations and were <20%.

Pharmacokinetic analyses

Analyses were conducted in BALB/c mice (Harlan, Indianapolis, IN) for MEDI-493 wild type, G385D/Q386P/N389S, M252Y/S254T/T256E, and H433K/N434F/Y436H, and were approved by MedImmune's Review Board. Each animal (10/group) was injected i.m. with 2.5 μg of protein in a volume of 100 μl of PBS. Mice were bled from the retro-orbital sinus for each time point. Data were collected every 24 h until day 5 postinjection and every 48 h thereafter until day 12. Urine and serum were also collected at 6 and 24 h post-i.m. injection of 30 μg of each IgG1 (two animals/group). Concentrations were determined by an anti-human IgG ELISA. Briefly, individual wells of a 96-well Maxisorp Immunoplate (Nunc) were coated with 50 ng of a goat anti-MEDI-493 (anti-idiotype) Ab (MedImmune). The plates were blocked with 0.5% (w/v) BSA (Sigma-Aldrich, St. Louis, MO), incubated with samples or standards (0.1–20 ng/ml), then with a HRP conjugate of a goat anti-human Fc polyclonal Ab (Sigma-Aldrich). Peroxidase activity was detected with 3,3′,5,5′-tetramethylbenzidine (Kirkegaard & Perry Laboratories, Gaithersburg, MD), and the reaction was quenched with 0.18 M H_2SO_4. The absorbance at 450 nm was measured with a V_{max} kinetic microplate reader running SoftMaxPro 3.1.1 software (Molecular Devices, Sunnyvale, CA). The $t_{1/2}$ of the elimination phase (β phase), which takes place after the rapid redistribution phase, were determined using a one-phase exponential decay model provided by GraphPad Prism (GraphPad Software, San Diego, CA), using data points between day 1 and 12 postinjection.

Immunoprecipitation and immunohistochemistry

Analyses were conducted in BALB/c mice for MEDI-493 wild type, M252Y/S254T/T256E, and H433K/N434F/Y436H. Using two mice per group, each animal was injected i.v. or i.m. with 30 μg of Ig in a volume of 100 μl of PBS or with 100 μl of PBS. After 24 h, animals were killed. Lungs, spleen, liver, intestine, heart, kidneys, bladder, as well as muscle at the site of i.m. injection were harvested.

Immunoprecipitation

Organs were removed into 1 ml PBS, ground, and lysed by sonication, and lysates were cleared by centrifugation. Immunoprecipitation was performed for 2 h at room temperature using 50 μl of a 50% suspension of goat anti-human IgG-Sepharose 4B conjugate (Zymed, South San Francisco, CA) previously washed three times with 1 ml triethylamine 100 mM, pH 11.0. Beads were washed three times with 1 ml PBS/0.1% Tween 20, pH 7.2, and elution was conducted in 50 μl 100 mM triethylamine, pH 11.0. Eluates were boiled for 5 min and loaded on a SDS-PAGE (4–20% gels; Invitrogen) in presence of 50 mM DTT. Electrotransfer to nitrocellulose filters was made as described (34). Detection was conducted with a HRP conjugate of a goat anti-human IgG (anti-Fab; Sigma-Aldrich) and the ECL Western blotting detection reagents (APBiotech).

Immunohistochemistry

Organs were removed into neutral buffered 10% Formalin solution (Sigma-Aldrich). Immunohistochemistry experiments were conducted at Molecular Histology (Gaithersburg, MD) on paraffin-embedded samples using a HRP conjugate of a goat anti-human IgG (anti-whole molecule; Sigma-Aldrich) and standard protocols (DAKO Handbook on Immunochemical Staining Methods; DAKO, Carpenteria, CA).

Phosphor imaging

Analyses were conducted in BALB/c mice. Briefly, MEDI-493 wild type, M252Y/S254T/T256E, and H433K/N434F/Y436H were radiolabeled with $Na^{125}I$ by the chloramine-T procedure (41) at Lofstrand Labs (Gaithersburg, MD) to a specific radioactivity of $\sim 5 \times 10^6$ dpm/μg. Using two mice per group, each animal was injected i.m. with 2.5 μg of iodinated Ig in a volume of 100 μl of PBS. After 24 h, animals were killed. Lungs, spleen, liver, intestine, and heart were harvested and transferred into neutral buffered 10% Formalin solution (Sigma-Aldrich). The radioactivity present was quantitated by phosphor imaging analysis after 3-wk exposure (42) using a Fuji BAS 5000 running Image Gauge V3.45.

Results

Phage display of human Fc fragments

Libraries of human hinge-Fc fragments (residues 226–478, Kabat numbering) (21) derived from the human IgG1 MEDI-493 (31) were expressed using the pCANTAB5E phagemid vector. As previously noted (11), functional Fc-hinge homodimers linked to the gene III coat protein are formed and displayed at the surface of M13 by virtue of the leakiness of the amber stop codon located between hinge-Fc:E-Tag and gene III.

Mutagenesis and selection

Four libraries (1, 2, 3, and 4) were constructed by Kunkel-based mutagenesis, which contained Fc variants with residues randomized at contact positions between Fc and murine or human FcRn.

A- Fc selected sequences

Library 1 (251-256)	Library 2 (308-314)	Library 3 (385-389)	Library 4 (428-436)
LMISRT(wt)	VLHQDWL(wt)	GQPEN(wt)	MHEALHNHY(wt)
LYITRE	TPHSDWL	RTREP	*MHEALRYHH*
LYISRT	IPHEDWL	*DPPES*	MHEALHFHH
LYISRS		SDPEP	MHEALKFHH
LYISRR		TSHEN	MHEALSYHR
LYISRQ		SKSEN	THEALHYHT
LWISRT		HRSEN	MHEALHYHY
LYISLQ		KIREN	
LFISRD		GITES	
LFISRT		SMAEP	
LFISRR			
LFITGA			
LSISRE			
RTISIS			

B- Residue occurence

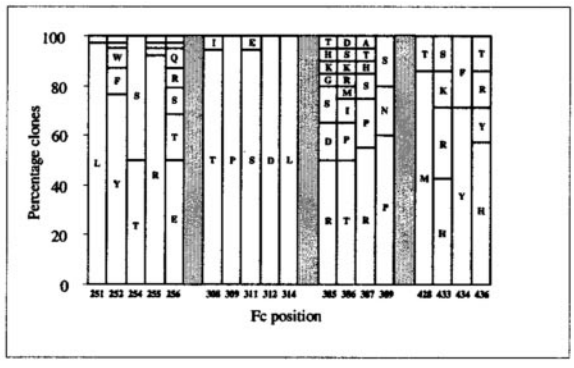

FIGURE 1. *A*, Fc sequences of phage clones identified after three (library 1, 2, and 4) or six (library 3) rounds of panning using murine FcRn. Residues in bold indicate fixed residues. Sequences underlined and in italic correspond to clones with an occurrence frequency of 10–20 times and of 2–5 times, respectively. *B*, Summary of the occurrence of selected residues at particular positions. The chart was generated by calculating the appearance frequency of the most commonly occurring residues at each randomized position.

Library 1 targeted positions 251, 252, and 254–256 (EU numbering) (21); library 2 positions 308, 309, 311, 312, and 314; library 3 positions 385, 386, 387, and 389; and library 4 positions 428, 433, 434, and 436. D312 and N389 are not predicted to contact murine or human FcRn, but due to their solvent-exposed nature as well as close proximity to the FcRn binding site, these residues were also randomized. Residues I253, H310, and H435 are highly conserved across species (21), play a major role in the energetics and pH specificity of binding to murine and human FcRn (8, 24, 29), and therefore were fixed during mutagenesis to retain the crucial functional epitope. To limit the size of the libraries and to avoid cumbersome sampling procedures, W313, E388, H429, E430, A431, and L432, which are not predicted to contact rat or human FcRn (16, 23), were also fixed. Libraries 1 and 2 consist of 1×10^8 clones each, representing a significant proportion of the 3.4×10^7 (32^5) possible codon permutations from the NNS randomization strategy. Likewise, libraries 3 and 4 of 1×10^7 clones each represented a significant proportion of the 1.0×10^6 (32^4) possible codon permutations. After three rounds of panning, a strong consensus sequence had emerged for libraries 1, 2, and 4 (Fig. 1), but not library 3. After six rounds of panning, a consensus sequence had appeared for library 3 (Fig. 1). Clones isolated from library 1 have predominantly L at position 251, Y at 252, T or S at 254, R at 255, and broader variability at 256 (Fig. 1*B*). Clones isolated from library 2 have predominantly T at position 308, P at 309, S at 311, D at 312, and L at 314 (Fig. 1*B*). Clones isolated from library 3 have more variability at every position, but predominantly R at position 385, T at 386, R at 387, and P at 389 (Fig. 1*B*). Clones isolated from library 4 have predominantly M at position 428, Y at 434, and broader specificity at other positions, with H, R, K, and S being frequently found at 433, and H, Y, R, and T at 436 (Fig. 1*B*).

SPR analyses

The ability of murine and human FcRn to bind the Fc variants was investigated using SPR (BIAcore). Representative mutations identified after panning libraries 1 through 4 (Fig. 1*A*) were introduced into the Fc portion of a human IgG1 (Table I). Injection of different concentrations of human or murine FcRn over the immobilized IgG1 variants gave concentration-dependent binding at pH 6.0. A typical resonance profile for equilibrium binding is shown for the M252Y/S254T/T256E mutant (Fig. 2, *A* and *B*). In all cases, equilibrium (or near-equilibrium) binding levels were reached within 50 min. The Scatchard plots for the binding of the M252Y/S254T/T256E mutant to murine and human FcRn are shown in Fig. 2, *C* and *D*. The plots were all linear, and apparent K_a were calculated from the relevant slopes. Measurements were conducted in duplicate or triplicate and confirmed that the immobilized IgGs retained their original binding activity.

Because there are two nonequivalent binding sites on human IgG for mouse/human FcRn (17, 43), the receptor was used in solution to avoid avidity effects. Consistent with this, systematically higher affinities are observed when FcRn, rather than IgG, is immobilized on the biosensor chip (17, 29, 44, 45). Under our experimental conditions, mainly interactions corresponding to the higher affinity association (i.e., single-liganded receptor) are measured, accounting for the linearity of the Scatchard plots.

Binding of the Fc mutants

The K_d for the interaction of wild-type human IgG1 with murine and human FcRn at pH 6.0 (269 and 2527 nM, respectively) agree well with the values determined by others (8). Our data (Table I) indicate that the I253A mutation virtually abolishes binding to human and murine FcRn, as reported previously (12, 24). This is not the result of misfolding of the Ab, as this mutant retains the same sp. act. as the wild-type molecule (MEDI-493) in a microneutralization assay (31) (data not shown).

We generated human IgG1 mutants with increased binding affinity toward both murine and human FcRn at pH 6.0 (Table I). Overall, improvements in complex stability were less marked for the human IgG1-human FcRn pair than for the human IgG1-murine FcRn pair. The largest observed increases in affinity for single Fc region mutants toward murine and human FcRn compared with wild-type IgG1 were 30 (N434F/Y436H)- and 11 (M252Y/S254T/T256E)-fold, respectively. However, ranking of the most critical positions remains unchanged when comparing human and murine

Table I. *Dissociation constants and relative free energy changes for the binding of IgG1/Fc mutants to murine and human FcRn*[a]

Mutant	Dissociation Constant Fc/Murine FcRn (nM)	ΔΔG (kcal/mol)	Dissociation Constant Fc/Human FcRn (nM)	ΔΔG (kcal/mol)
Wild type	269 ± 1	NA	2527 ± 117	NA
I253A	NB	NA	NB	NA
M252Y/S254T/T256E	27 ± 6	1.4	225 ± 10	1.4
M252W	30 ± 1	1.3	408 ± 24	1.1
M252Y	41 ± 7	1.1	532 ± 37	0.9
M252Y/T256Q	39 ± 8	1.1	560 ± 102	0.9
M252F/T256D	52 ± 9	1.0	933 ± 170	0.6
V308T/L309P/Q311S	153 ± 23	0.3	1964 ± 84	0.1
G385D/Q386P/N389S	187 ± 10	0.2	2164 ± 331	0.1
G385R/Q386T/P387R/N389P	147 ± 24	0.4	1620 ± 61	0.3
H433K/N434F/Y436H	14 ± 2	1.8	399 ± 47	1.1
N434F/Y436H	9 ± 1	2.0	493 ± 7	1.0
H433R/N434Y/Y436H	14 ± 1	1.8	472 ± 61	1.0
[M252Y/S254T/T256E-H433K/N434F/Y436H]	9 ± 1	2.0	44 ± 3	2.4
[M252Y/S254T/T256E-G385R/Q386T/P387R/N389P]	28 ± 3	1.3	243 ± 48	1.4

[a] Affinity measurements were carried out by BIAcore, as described in *Materials and Methods*. Residue numbering is according to EU (21). The free energy change of dissociation, ΔG, is calculated as follows: $\Delta G = -R.T.1n[K_d]$, in which R is the gas constant, T is the absolute (Kelvin) temperature, and K_d is the dissociation constant. Differences in free energy changes are calculated as the differences between the ΔGs of wild-type and mutant reactions ($\Delta\Delta G = \Delta G_{wild\ type} - \Delta G_{mutant}$). NB, no binding; NA, nonapplicable.

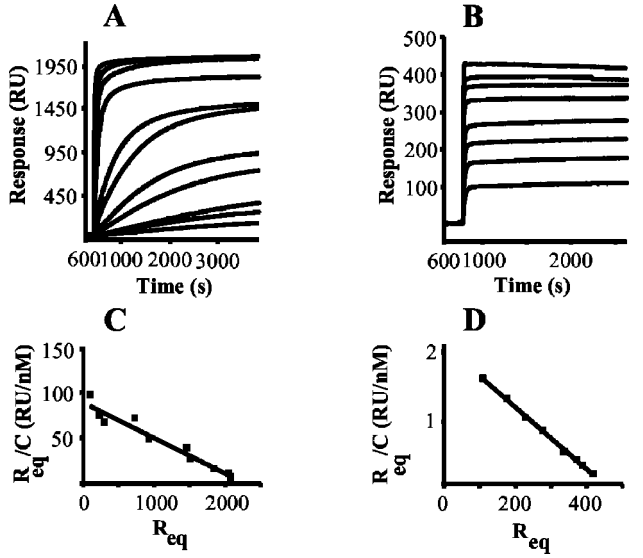

FIGURE 2. *A*, Binding of murine FcRn to immobilized M252Y/S254T/T256E. Murine FcRn was injected at 11 different concentrations ranging from 1 to 556 nM over a surface on which 4000 RU of IgG1 had been coupled. *B*, Binding of human FcRn to immobilized M252Y/S254T/T256E. Human FcRn was injected at eight different concentrations ranging from 71 nM to 2.86 μM over a surface on which 1000 RU of IgG1 had been coupled. *C* and *D*, Scatchard analysis of the data in *A* and *B*, respectively, after correction for nonspecific binding. R_{eq} is the corrected equilibrium response at a given concentration C. The plots are linear with correlation coefficients of 0.97 and 0.998, respectively. The apparent K_d are 24 and 225 nM, respectively.

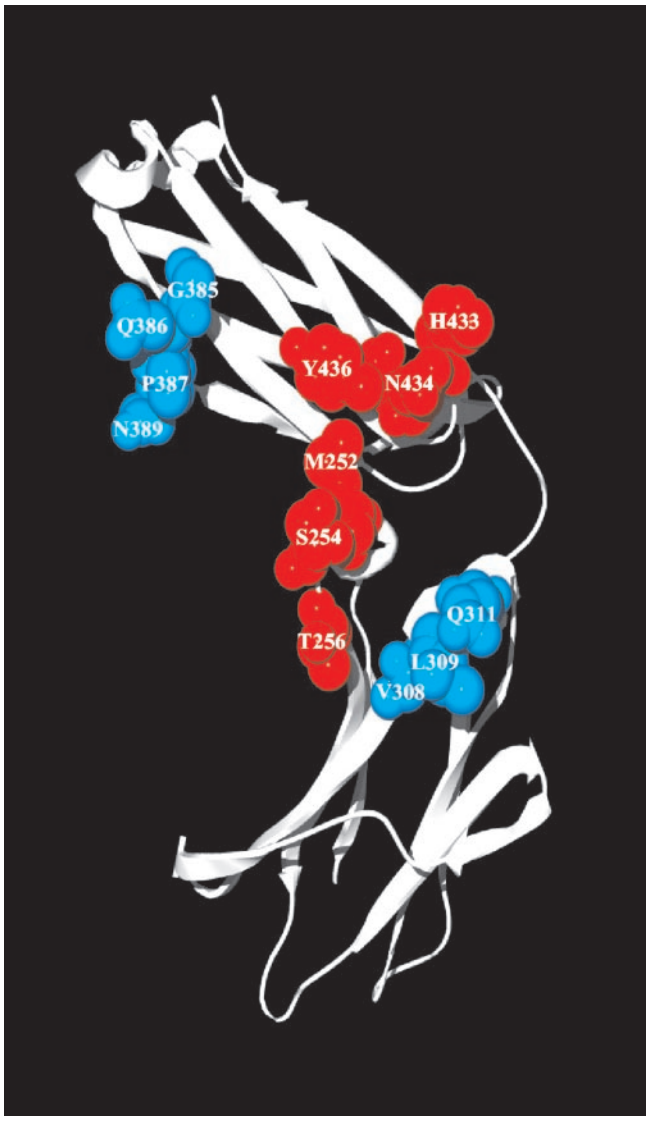

FIGURE 3. Space-filling model of the surface of the Fc fragment of a human IgG1 based upon the structure of a human IgG1 (47). The Fc fragment is oriented such that its docking surface with FcRn is pointing toward the reader. Residues are color coded according to the gain of free energy of stabilization of the Fc-FcRn complex: red, substitutions at those positions resulted in at least a 2.5- and 5-fold affinity increase to human and mouse FcRn, respectively; blue, substitutions at those positions were found to increase affinity by a factor of less than 2-fold in both the Fc-human FcRn and Fc-mouse FcRn interaction. The figure was drawn using Swiss pdb viewer (48).

FcRn: the largest increases in IgG1-murine FcRn complex stability ($\Delta\Delta G \geq 1.3$ kcal/mol) occurred for mutations at positions 252, 254, and 256 (M252Y/S254T/T256E and M252W) and 433, 434, and 436 (H433K/N434F/Y436H and N434F/Y436H). Likewise, the same mutations were found to have the most profound impact on the IgG1-human FcRn interaction and also resulted in the largest increases in complex stability ($\Delta\Delta G \geq 1.0$ kcal/mol). Substitutions at positions 308, 309, 311, 385, 386, 387, and 389 had little or no effect on the stability of the complexes involving human or murine FcRn ($\Delta\Delta G \leq 0.4$ kcal/mol). Therefore, residues at the center of the Fc-FcRn combining site contribute significantly more to improvement in complex stability than residues at the periphery (Fig. 3). Two combination variants were tested in which two Fc regions were simultaneously substituted. When tested against human FcRn, M252Y/S254T/T256E/H433K/N434F/Y436H shows an additive effect and exhibits binding that is better than M252Y/S254T/T256E and H433K/N434F/Y436H, but does not bind significantly better than H433K/N434F/Y436H to murine FcRn. M252Y/S254T/T256E/G385R/Q386T/P387R/N389P does not show any additive effect, as binding to both murine and human FcRn is not significantly different from M252Y/S254T/T256E.

Phage-derived IgG1 mutants exhibiting a significant increase in affinity toward murine FcRn at pH 6.0 ($\Delta\Delta G \geq 1.0$ kcal/mol) showed a parallel significant increase in binding to the mouse receptor at pH 7.4 (SPR $\text{signal}_{\text{pH 7.4}}$/SPR $\text{signal}_{\text{pH 6.0}}$ ~0.5 at equilibrium; Fig. 4, *C* and *D*). IgG1 mutants exhibiting a small increase in affinity toward murine FcRn at pH 6.0 ($\Delta\Delta G < 0.4$ kcal/mol) bound poorly to the mouse receptor at pH 7.4 (Fig. 4*B*). Raising the pH to 8.5 resulted in a dramatically lower binding of the mutants to murine FcRn when compared with at pH 6.0 and 7.4 (Fig. 4, *A–D*). In contrast, IgG1 mutants exhibiting a large affinity increase toward human FcRn at pH 6.0 ($\Delta\Delta G$ up to 1.4 kcal/mol) only showed minimal binding to the human receptor at pH 7.4 (SPR $\text{signal}_{\text{pH 7.4}}$/SPR $\text{signal}_{\text{pH 6.0}} < 0.1$ at equilibrium; Fig. 4, *G* and *H*). Only M252Y/S254T/T256E/H433K/N434F/Y436H ($\Delta\Delta G = 2.4$ kcal/mol at pH 6.0) bound significantly to human FcRn at pH 7.4 (SPR $\text{signal}_{\text{pH 7.4}}$/SPR $\text{signal}_{\text{pH 6.0}} = 0.45$ at equilibrium; unpublished observations). None of the variants tested bound at a detectable level to human FcRn at pH 8.5.

Pharmacokinetic studies

To correlate magnitude of the increase in affinity of the Fc-FcRn interaction with biological consequences, three IgG1 mutants were selected for pharmacokinetic studies. Those display large (M252Y/S254T/T256E and H433K/N434F/Y436H) to small (G385D/Q386P/N389S) increases in affinity toward both murine and human FcRn. The pharmacokinetics of MEDI-493 wild type,

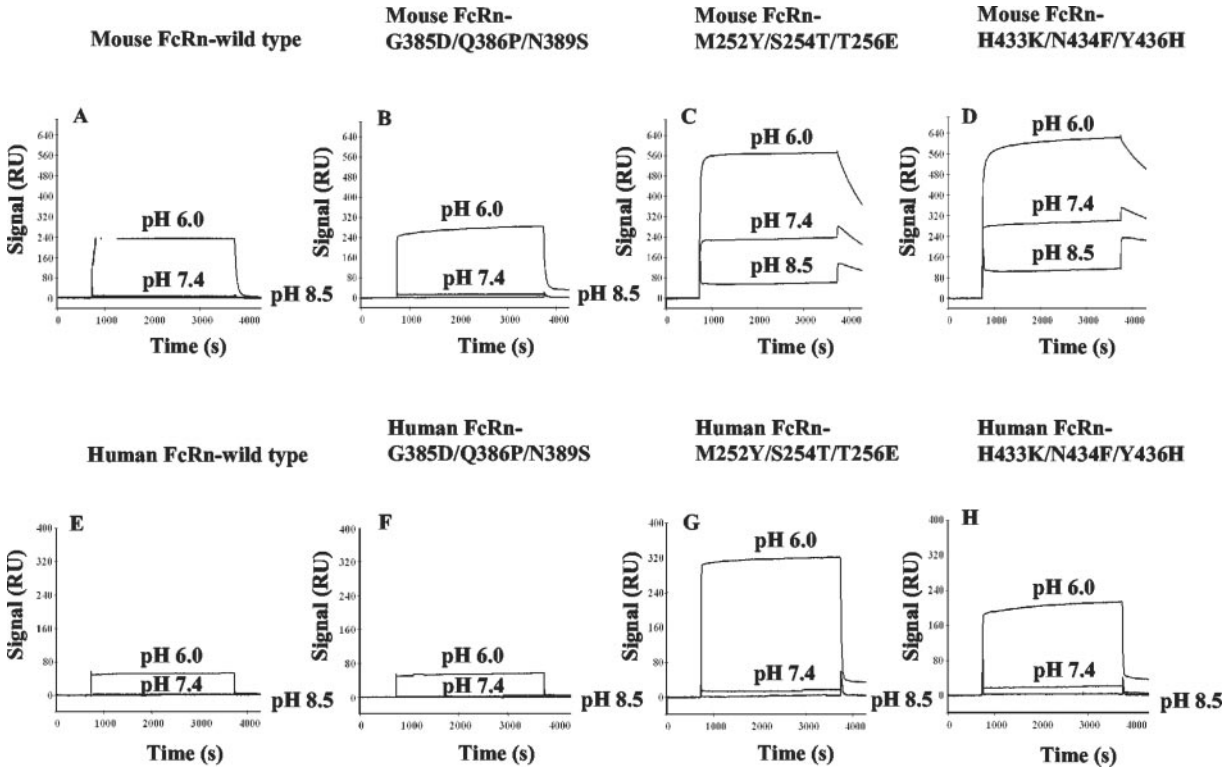

FIGURE 4. *A–D*, BIAcore analysis of the binding of murine FcRn at pH 6.0, 7.4, and 8.5 to wild-type human IgG1, G385D/Q386P/N389S, M252Y/S254T/T256E, and H433K/N434F/Y436H, respectively, after correction for nonspecific binding. Murine FcRn was injected at a concentration of 1 μM over a surface on which ~1000 RU of IgGs had been coupled. *E–H*, BIAcore analysis of the binding of human FcRn at pH 6.0, 7.4, and 8.5 to wild-type human IgG1, G385D/Q386P/N389S, M252Y/S254T/T256E, and H433K/N434F/Y436H, respectively, after correction for nonspecific binding. Human FcRn was injected at a concentration of 1 μM over a surface on which ~1000 RU of IgGs had been coupled.

G385D/Q386P/N389S, M252Y/S254T/T256E, and H433K/N434F/Y436H were analyzed in BALB/c mice. Those molecules were injected in equal amounts into different mice, and their serum concentration (reported in $ng_{variant/wild\ type}/ml_{serum}$) was determined by ELISA (see *Materials and Methods*). We report an inverse correlation between the binding affinity of the IgG1 variants to murine FcRn at pH 6.0 and their serum concentration (Fig. 5). M252Y/S254T/T256E and G385D/Q386P/N389S show significantly lower than wild-type serum concentrations starting at day 1 post-i.m. injection of 2.5 μg/animal of IgG1, whereas H433K/N434F/Y436H is virtually undetectable at the same time point (Fig. 5). Similar clearance results were obtained after i.v. injection of 2.5 μg/animal of IgG1 (data not shown). The same trends are observed after i.v. or i.m. injection of a >10-fold higher amount (30 μg/animal) of H433K/N434F/Y436H and M252Y/S254T/T256E as early as 6 h postinjection (Fig. 6). This is not the result of an enhanced degradation of the variants by serum or blood cell-associated proteases or of denaturation, as they have the same ex vivo stability in mouse serum and whole blood as the wild-type IgG1 for 24 h at 37°C, as determined by an anti-human IgG ELISA requiring the simultaneous presence of both a functional idiotope and Fc region (see *Materials and Methods*, data not shown). The same assay did not detect MEDI-493 wild type, M252Y/S254T/T256E, or H433K/N434F/Y436H in urine. Although the IgG1

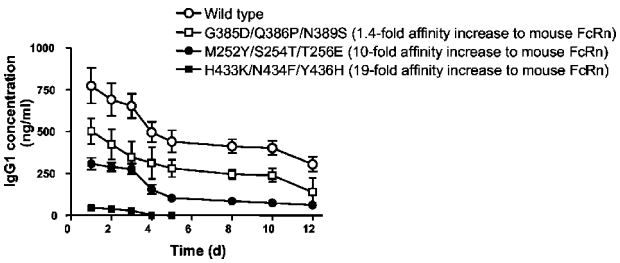

FIGURE 5. Clearance curves of human IgG1 wild type, G385D/Q386P/N389S (1.4-fold affinity increase to mouse FcRn), M252Y/S254T/T256E (10-fold affinity increase to mouse FcRn), and H433K/N434F/Y436H (19-fold affinity increase to mouse FcRn) following i.m. injection of 2.5 μg IgG1 in BALB/c mice. Each time point represents the average serum concentration for 10 mice. SDs are indicated by error bars.

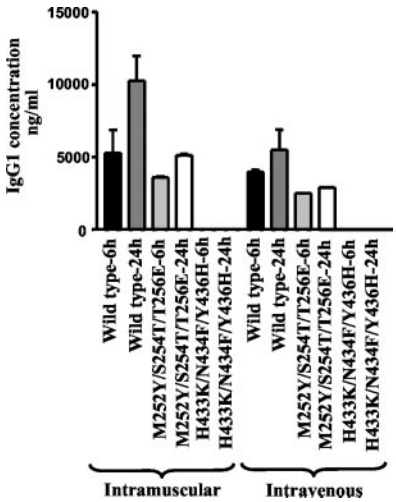

FIGURE 6. Serum concentrations of human IgG1 wild type, M252Y/S254T/T256E, and H433K/N434F/Y436H 6 and 24 h postinjection of 30 μg IgG1 in BALB/c mice. SDs are indicated by error bars.

Table II. *Pharmacokinetics of wild-type and mutant human IgG1 molecules in BALB/c mice*[a]

Human IgG1	No. of Mice	β Phase $t_{1/2}$ (d)
Wild type	10	3.2 ± 0.5
G385D/Q386P/N389S	10	2.8 ± 0.4
M252Y/S254T/T256E	10	3.0 ± 0.5

[a] Measurements were carried out, as described in *Materials and Methods*. Error was estimated as the SD for two independent series of measurements using MEDI-493 (wild type) IgG1.

variants we tested exhibit lower serum concentration when compared with wild type, β phase $t_{1/2}$ are not significantly different for MEDI-493 wild type, G385D/Q386P/N389S, and M252Y/S254T/T256E (Table II). The relationship, if any, between serum concentrations and β phase $t_{1/2}$ is at present unclear.

Immunoprecipitation

Presence of MEDI-493 wild type, M252Y/S254T/T256E, and H433K/N434F/Y436H was investigated by immunoprecipitation of different organs and tissue (lungs, spleen, intestine, heart, kidney, bladder, and site of i.m. injection) using an anti-human IgG conjugate. Muscle tissue at the site of injection revealed two polypeptide chains with apparent molecular mass ~50 and ~30 kDa, corresponding to the H and L chains, respectively, of MEDI-493 wild type, M252Y/S254T/T256E, and H433K/N434F/Y436H (Fig. 7). No significant difference could be observed between the three IgGs. Those molecules could not be detected in lungs, spleen, intestine, heart, kidney, or bladder after i.m. or i.v. injection. Those results indicate that no enhanced retention or degradation of the mutants is taking place in muscle tissue. In agreement with those data, immunohistochemistry on lungs, spleen, liver, intestine, heart, kidney, and bladder did not reveal any significant amounts of M252Y/S254T/T256E and H433K/N434F/Y436H (unpublished observations).

Phosphor imaging

To more accurately determine the concentrations of MEDI-493 wild type, M252Y/S254T/T256E, and H433K/N434F/Y436H in different organs, a more sensitive detection assay was used in which IgG1s were iodinated and i.m. injected in BALB/c mice. Different tissues were then submitted to a phosphor imaging analysis. It revealed that MEDI-493 wild type is found at the highest levels in lungs, spleen, heart, and liver. Intestine exhibits lower levels. M252Y/S254T/T256E and H433K/N434F/Y436H follow the same trend, but at significantly lower concentrations overall than MEDI-493 wild type (Table III, Fig. 8). Those results indicate that no significant enhanced retention of the mutants is taking place in the organs tested. No conclusion pertaining to the degradation rate of the mutants in those organs can be formulated because the lower-than-wild-type organ concentrations might just reflect the overall lower serum concentrations.

Discussion

In this study, we have demonstrated that the stability of the complex between murine or human FcRn with a human IgG1 can be increased by >30-fold by screening libraries of randomized Fc residues. Four libraries were designed that targeted Fc residues in contact with, or in close proximity of, the α1/α2 domains of murine and human FcRn (1, 15, 16, 23). These Fc libraries introduced substitutions in three loops at the CH_2-CH_3 junction (strands B and E of CH_2, and G of CH_3) and in one region between strands C and D of CH_3.

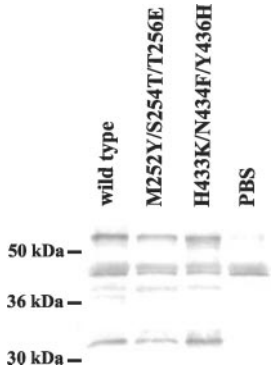

FIGURE 7. Immunoprecipitation of human IgG1 wild type, M252Y/S254T/T256E, and H433K/N434F/Y436H in muscle 24 h post-i.m. injection of 30 μg IgG1 in BALB/c mice.

Engineering of the Fc-FcRn interaction indicates that major improvements in murine FcRn-human IgG1 and human FcRn-human IgG1 complex stability (0.6 kcal/mol $\leq \Delta\Delta G \leq$ 2.4 kcal/mol) occur on substituting residues located in a band across the Fc-FcRn interface (M252, S254, T256, H433, N434, and Y436). Substitutions of residues at the periphery (V308, L309, Q311, G385, Q386, P387, and N389) resulted in little or no increase in the free energy of complex stabilization ($\Delta\Delta G \leq$ 0.4 kcal/mol). V308T/L309P/Q311S, G385R/Q386T/P387R/N389P, and, to a lesser extent, G385D/Q386P/N389S were strongly selected for (Fig. 1, *A* and *B*), but did not exhibit a marked increase in affinity toward both murine and human FcRn ($\Delta\Delta G \leq$ 0.4 kcal/mol). This suggests that the two peripheral FcRn-contacting regions are not suitable targets for the engineering of IgGs with significant increases in affinity for FcRn. This might reflect the hot spot nature of the central region. In this situation, the energy of stabilization arises primarily from a few residues located at the center of a protein-protein interface (40). In fact, central residues I253 and H435 have already been shown to be critical to formation of the complex between human Fc and murine FcRn (12), and I253, S254, H435, and Y436 play a crucial role in the interaction of human IgG1 with human FcRn (8, 24). Thus, proximity of a pre-existing hot spot might be an important criteria to consider when engineering mutants for improved binding activity. However, H310 has been shown to be part of the energetic epitope for both human and murine FcRn, and yet mutations in its vicinity did not yield any variant with improvement in affinity above 1.7-fold. More likely is that additional factors around the substituted residue, such as the local chemical microenvironment, protein conformational changes, as well as solvent reorganization, have to be taken into account. Alternatively, the observed pattern might reflect other factors, such as library design, incomplete library sampling, and inefficient selection of more favorable residues at the peripheral positions due to a decrease in Fc stability or less efficient display at the surface of M13.

Interestingly, the variant with the highest affinity to human FcRn was obtained by combining the M252Y/S254T/T256E and H433K/N434F/Y436H mutations and exhibited a 57-fold increase in affinity relative to the wild-type IgG1. In comparison, both single substitutions resulted in only an 11- and 6.5-fold improvement in binding to human FcRn, respectively, as compared with wild-type IgG1. In contrast, the combination of M252Y/S254T/T256E with G385R/Q386T/P387R/N389P did not result in further affinity improvement toward human FcRn relative to M252Y/S254T/T256E. This confirms the dominance of the central over the peripheral residues in the energetics of the complex formation.

Efficient binding of human Fc to murine FcRn at pH 6.0 requires the presence of several wild-type Fc residues. For example, leucine

Table III. *Phosphor imaging of ^{125}I for wild-type and mutant human IgG1 molecules in BALB/c mice*[a]

Mutant	Liver PSL/mm^2[b]	Lung PSL/mm^2	Heart PSL/mm^2	Spleen PSL/mm^2	Small Intestine PSL/mm^2	Large Intestine PSL/mm^2
Wild type	117 ± 36	121 ± 37	123 ± 10	114 ± 6	35 ± 7	51 ± 6
M252Y/S254T/T256E	35 ± 3	29 ± 5	30 ± 6	27 ± 1	ND	ND
H433K/N434F/Y436H	13 ± 1	12 ± 1	12 ± 1	12 ± 1	ND	ND

[a] Measurements were carried out, as described in *Materials and Methods*, at Molecular Histology. Error was estimated as the SD for two independent series of measurements.

[b] Photo-stimulated luminescence (PSL) density. ND, not determined due to low signal. Background slide reading was 10.7 PSL/mm^2. Background plate reading was 9.1 PSL/mm^2.

is very conserved at 251, arginine at 255, aspartic acid at 312, leucine at 314, and methionine at 428 (Fig. 1). Retention of those wild-type residues indicates they are the most favorable for efficient binding to murine FcRn. These amino acids are well conserved in human and murine IgGs (21). In particular, D312 is not predicted to contact human or murine FcRn, and conservation of this residue in the phage-derived clones suggests that it has an important, but indirect role in the energetics of association with murine FcRn. Alternative explanations include biases in the library or incomplete sampling.

Another specificity trend is observed when one considers positions 308, 309, and 311 in which threonine, proline, and serine, respectively, are very strongly favored over the corresponding wild-type residues (Fig. 1). Surprisingly, this does not correlate with the magnitude of increase in affinity, as V308T/L309P/Q311S binds less than 2-fold better than the wild-type IgG1 to both human and murine FcRn (Table I). There appears to be a selection for residues with an aromatic side chain at position 252 (Y, F, and W). Engineering of the interaction of murine Fc fragments with murine FcRn has already revealed that a leucine at this position is the most favorable residue (11). No clones were found in our experiments that contained a leucine at 252. This difference might reflect the distinct local environment present in both murine and human Fc.

The three-dimensional structure of human and rodent FcRn is very similar (17). However, there are a number of differences at the interface of contact with Fc, the most notable of which is a substitution of L135 (human) for D137 (mouse). Our selection results indicate a strong trend toward conservation of H and selection of K and R at position 433 as well as toward selection of H and R at position 436. This underlines the importance of a positively charged residue at those locations. Interestingly, histidine at position 436 is highly conserved in murine IgG1 sequences, in which it is thought to interact through a salt bridge with murine FcRn D137 (23). In contrast, tyrosine at position 436 is conserved in human IgG1 sequences, in which it is believed to make hydrophobic interactions with human FcRn L135. Selection of H436 after selection of random human Fc libraries on murine FcRn probably recreates the important interaction with D137. This is supported by the 30-fold increase in the affinity of N434F/Y436H for murine FcRn compared with wild type. Elucidation of the molecular mechanisms by which human FcRn not only accommodates a histidine at position 436, but also has enhanced binding to N434F/Y436H will require a more detailed analysis, such as the construction of additional mutants and x-ray crystallography.

Surprisingly, efforts to use human FcRn for screening the libraries were not successful due to the lack of consensus sequences after seven rounds of panning. A likely explanation is that the selection conditions we tested were detrimental to its stability and/or function. As a result, libraries were panned against murine FcRn, with a binding step at pH 6.0 and an elution step at pH 7.4. This strategy allowed direct isolation of clones that bound more tightly at pH 6.0 than at pH 7.4. However, there was a marked difference in the effect of pH on the binding of the IgG1 variants to either human or murine FcRn. Increases in the stability of the complex with murine FcRn at pH 6.0 correlate with increases in the stability of the complex at pH 7.4 (Fig. 4, *A–D*). In contrast, most IgG1 mutants bound very poorly to human FcRn at pH 7.4 (Fig. 4*E–H*). In all cases, binding was dramatically decreased

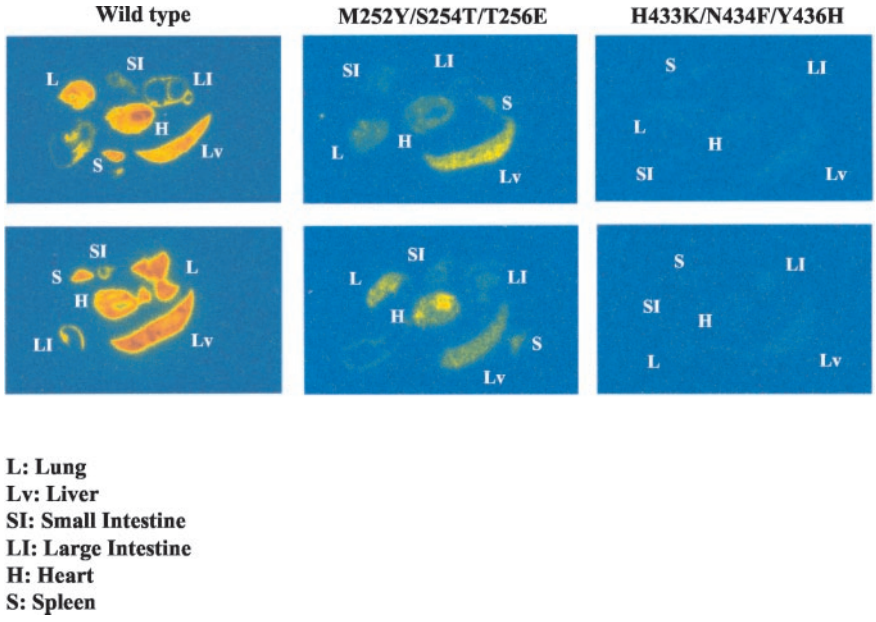

FIGURE 8. Phosphor imaging of ^{125}I in lung, liver, spleen, intestine, and heart for human IgG1 wild type, M252Y/S254T/T256E, and H433K/N434F/Y436H 24 h post-i.m. injection of 2.5 μg iodinated IgG1 in BALB/c mice.

when pH was raised to 8.5, strongly suggesting the mutations we identified led to a change in the pKa of H310 and/or H435, which are responsible for the pH dependency of binding (23). This has clear implications for the pharmacokinetics of the IgG1 variants, as higher affinity to FcRn at pH 7.4 might adversely affect release into the serum and offset the benefit of the enhanced binding at pH 6.0. Our pharmacokinetic and immunohistochemistry studies in mice support this hypothesis because serum levels after i.m. or i.v. injection were consistently lower for G385D/Q386P/N389S, M252Y/S254T/T256E, and H433K/N434F/Y436H when compared with the wild-type molecule. Those mutants are also present at lower levels in different tissues when compared with wild type. No evidence of enhanced degradation in serum, blood, or muscle tissue at the site of injection was found. Likewise, there was no detectable enhanced excretion in urine. It is possible to hypothesize that because of their more efficient binding at pH 7.4, the IgG1 mutants are sequestered throughout the body in FcRn-containing tissues such as the endothelium of small arterioles and capillaries (20). Retention of the IgGs in cells may lead to their degradation. This may not be an issue in humans because the majority of the IgG1 mutants we tested do not bind well to human FcRn at pH 7.4 when compared at pH 6.0. If this hypothesis is correct, introduction of the mutations we identified into the Fc fragment of therapeutic Abs may increase their serum persistence.

Enhancements of the affinity of our human IgG variants for both human and murine FcRn are anticipated from further engineering, such as the randomization of new sets of residues and the selection of the best combinations of mutations by DNA shuffling (46). Those studies will yield important information pertaining to the molecular basis of protein-protein interactions. Provided retention of the pH dependency of binding can be conserved, it might be possible to generate IgG mutants exhibiting enhanced efficacy due to long serum $t_{1/2}$. Those molecules could be a valuable addition to the therapeutic Ab field and have potential utility in domains as diverse as cancer, respiratory diseases, neonatal medicine, and diagnostic.

Acknowledgments

We thank Fran Palmer-Hill, Mary Bladen, James Johnson, and Jing Tan for expert technical assistance.

References

1. Ghetie, V., and S. Ward. 2000. Multiple roles for the major histocompatibility complex class I-related receptor FcRn. *Annu. Rev. Immunol. 18:739.*
2. Wallace, K. H., and A. R. Rees. 1980. Studies on the immunoglobulin-G Fc-fragment receptor from neonatal rat small intestine. *Biochem. J. 188:9.*
3. Medesan, C., C. Radu, J. K. Kim, V. Ghetie, and S. Ward. 1996. Localization of the site of the IgG that regulates maternofetal transmission in mice. *Eur. J. Immunol. 26:2533.*
4. Cianga, P., C. Medesan, J. Richardson, V. Ghetie, and E. S. Ward. 1999. Identification and function of neonatal Fc receptor in mammary gland of lactating mice. *Eur. J. Immunol. 29:2515.*
5. Ghetie, V., J. G. Hubbard, J. K. Kim, M. F. Tsen, Y. Lee, and E. S. Ward. 1996. Abnormally short serum half lives of IgG in β_2-microglobulin-deficient mice. *Eur. J. Immunol. 26:690.*
6. Junghans, R. P., and C. L. Anderson. 1996. The protection receptor for IgG catabolism is the β_2-microglobulin-containing neonatal intestinal transport receptor. *Proc. Natl. Acad. Sci. USA 93:5512.*
7. Story, C. M., J. E. Mikulska, and N. E. Simister. 1994. A major histocompatibility complex class 1-like Fc receptor cloned from human placenta: possible role in transfer of immunoglobulin G from mother to fetus. *J. Exp. Med. 180:2377.*
8. Firan, M., R. Bawdon, C. Radu, R. J. Ober, D. Eaken, F. Antohe, V. Ghetie, and S. Ward. 2001. The MHC class I-related receptor, FcRn, plays an essential role in the maternofetal transfer of γ-globulin in humans. *Int. Immunol. 13:993.*
9. Israel, E. J., S. Taylor, Z. Wu, E. Mizoguchi, R. S. Blumberg, A. Bhan, and N. E. Simister. 1997. Expression of the neonatal Fc receptor, FcRn, on human intestinal epithelial cells. *Immunology 92:69.*
10. Dickinson, B. L., K. Badizadegan, Z. Wu, J. C. Ahouse, X. Zhu, N. E. Simister, R. S. Blumberg, and W. I. Lencer. 1999. Bidirectional FcRn-dependent IgG transport in a polarized human intestinal epithelial cell line. *J. Clin. Invest. 104:903.*
11. Ghetie, V., S. Popov, J. Borvak, C. Radu, D. Matesoi, C. Medesan, R. Ober, and S. Ward. 1997. Increasing the serum persistence of an IgG fragment by random mutagenesis. *Nat. Biotechnol. 15:637.*
12. Kim, J. K., M. Firan, C. Radu, C. H. Kim, V. Ghetie, and S. Ward. 1999. Mapping the site on human IgG for binding of the MHC class I-related receptor, FcRn. *Eur. J. Immunol. 29:2819.*
13. Simister, N. E., and K. E. Mostov. 1989. An Fc receptor structurally related to MHC class I antigens. *Nature 337:184.*
14. Ahouse, J. J., C. L. Hagerman, P. Mittal, D. J. Gilbert, N. G. Copeland, N. A. Jenkins, and N. E. Simister. 1993. Mouse MHC class I-like Fc receptor encoded outside the MHC. *J. Immunol. 151:6076.*
15. Burmeister, W. P., L. N. Gastinel, N. E. Simister, M. L. Blum, and P. J. Bjorkman. 1994. Crystal structure at 2.2 Å resolution of the MHC-related neonatal Fc receptor. *Nature 372:336.*
16. Burmeister, W. P., A. H. Huber, and P. J. Bjorkman. 1994. Crystal structure of the complex of rat neonatal Fc receptor with Fc. *Nature 372:379.*
17. West, A. P., and P. J. Bjorkman. 2000. Crystal structure and immunoglobulin G binding properties of the human major histocompatibility complex-related Fc receptor. *Biochemistry 39:9698.*
18. Rodewald, R. 1976. pH-dependent binding of immunoglobulins to intestinal cells of the neonatal rat. *J. Cell Biol. 71:666.*
19. Kristoffersen, E. K., and R. Matre. 1996. Co-localization of the neonatal Fcγ receptor and IgG in human placental term syncytiotrophoblasts. *Eur. J. Immunol. 26:1668.*
20. Borvak, J., J. Richardson, C. Medesan, F. Antohe, C. Radu, M. Simionescu, V. Ghetie, and E. S. Ward. 1998. Functional expression of the MHC class I-related receptor, FcRn, in endothelial cells of mice. *Int. Immunol. 10:1289.*
21. Kabat, E. A., T. T. Wu, H. M. Perry, K. S. Gottesman, and C. Foeller. 1991. *Sequences of Proteins of Immunological Interest*. U.S. Public Health Service, National Institutes of Health, Bethesda, MD.
22. Kim, J. K., M. F. Tsen, V. Ghetie, and S. Ward. 1994. Identifying amino acid residues that influence plasma clearance of murine IgG1 fragments by site-directed mutagenesis. *Eur. J. Immunol. 24:542.*
23. Martin, W. L., A. P. West, L. Gan, and P. J. Bjorkman. 2001. Crystal structure at 2.8Å of an FcRn/heterodimeric Fc complex: mechanism of pH-dependent binding. *Mol. Cell 7:867.*
24. Shields, R. L., A. K. Namenuk, K. Hong, Y. G. Meng, J. Rae, J. Briggs, D. Xie, J. Lai, A. Stadlen, B. Li, et al. 2001. High resolution mapping of the binding site on human IgG1 for FcγRI, FcγRII, FcγRIII, and FcRn and design of IgG1 variants with improved binding to the FcγR. *J. Biol. Chem. 276:6591.*
25. Raghavan, M., M. Y. Chen, L. N. Gastinel, and P. J. Bjorkman. 1994. Investigation of the interaction between the class I MHC-related Fc receptor and its immunoglobulin G ligand. *Immunity 1:303.*
26. Vaughn, D. E., C. M. Milburn, D. M. Penny, W. L. Martin, J. L. Johnson, and P. J. Bjorkman. 1997. Identification of critical IgG binding epitopes on the neonatal Fc receptor. *J. Mol. Biol. 274:597.*
27. Chintalacharuvu, K. R., L. C. Vuong, L. A. Loi, J. W. Larrick, and S. L. Morrison. 2001. Hybrid IgA2/IgG1 antibodies with tailor-made effector functions. *Clin. Immunol. 101:21.*
28. Raghavan, M., V. R. Bonagura, S. L. Morrison, and P. J. Bjorkman. 1995. Analysis of the pH dependence of the neonatal Fc receptor/immunoglobulin G interaction using antibody and receptor variants. *Biochemistry 34:14649.*
29. Popov, S., J. G. Hubbard, J. Kim, B. Ober, V. Ghetie, and E. S. Ward. 1996. The stoichiometry and affinity of the interaction of murine Fc fragments with the MHC class I-related receptor, FcRn. *Mol. Immunol. 33:521.*
30. Medesan, C., P. Cianga, M. Mummert, D. Stanescu, V. Ghetie, and E. S. Ward. 1998. Comparative studies of rat IgG to further delineate the Fc:FcRn interaction site. *Eur. J. Immunol. 28:2092.*
31. Johnson, S., C. Oliver, G. A. Prince, V. G. Hemming, D. S. Pfarr, S. C. Wang, M. Dormitzer, J. O'Grady, S. Koenig, J. K. Tamura, et al. 1997. Development of a humanized monoclonal antibody (MEDI-493) with potent in vitro and in vivo activity against respiratory syncytial virus. *J. Infect. Dis. 176:1215.*
32. Kunkel, T. A., J. D. Roberts, and R. A. Zakour. 1987. Rapid and efficient site-specific mutagenesis without phenotypic selection. *Methods Enzymol. 154:367.*
33. Ho, S. N., H. D. Hunt, R. M. Horton, J. K. Pullen, and L. R. Pease. 1989. Site-directed mutagenesis by overlap extension using the polymerase chain reaction. *Gene 15:51.*
34. Sambrook, J., E. F. Fritsch, and T. Maniatis. 1989. *Molecular Cloning: A Laboratory Manual*, Vols. 1, 2, and 3. Cold Spring Harbor Laboratory Press, Cold Spring Harbor.
35. Marks, J. D., H. R. Hoogenboom, T. P Bonnett, J. McCafferty, A. D. Griffiths, and G. Winter. 1991. Bypassing immunization: human antibodies from V-gene libraries displayed on phage. *J. Mol. Biol. 222:581.*
36. Sanger, F., S. Nicklen, and A. R. Coulson. 1977. DNA sequencing with chain-terminating inhibitors. *Proc. Natl. Acad. Sci. USA 74:5463.*

37. Van der Merwe, P. A., A. N. Barclay, D. W. Mason, E. A. Davies, B. P. Morgan, M. Tone, A. K. C. Krishnam, C. Ianelli, and S. J. Davis. 1994. Human cell-adhesion molecule CD2 binds CD58 (LFA-3) with a very low affinity and an extremely fast dissociation rate but does not bind CD48 or CD59. *Biochemistry 33:10149.*
38. Van der Merwe, P. A., M. H. Brown, S. J. Davis, and A. N. Barclay. 1993. Affinity and kinetic analysis of the interaction of the cell adhesion molecules rat CD2 and CD48. *EMBO J. 12:4945.*
39. Johnsson, B., S. Lofas, and G. Lindquist. 1991. Immobilization of proteins to a carboxymethyldextran-modified gold surface for biospecific interaction analysis in surface plasmon resonance sensors. *Anal. Biochem. 198:268.*
40. Dall'Acqua, W., E. R. Goldman, E. Eisenstein, and R. A. Mariuzza. 1996. A mutational analysis of the binding of two different proteins to the same antibody. *Biochemistry 35:9667.*
41. Hunter, W. M., and F. C. Greenwood. 1962. Preparation of iodine-131 labelled human growth hormone of high specific activity. *Nature 194:495.*
42. Johnston, R. F., S. C. Pickett, and D. L. Barker. 1990. Autoradiography using storage phosphor technology. *Electrophoresis 11:355.*
43. Sanchez, L. M., D. M. Penny, and P. J. Bjorkman. 1999. Stoichiometry of the interaction between the major histocompatibility complex-related Fc receptor and its Fc ligand. *Biochemistry 38:9471.*
44. Martin, W. L., and P. J. Bjorkman. 1999. Characterization of the 2:1 complex between the class I-related Fc receptor and its Fc ligand in solution. *Biochemistry 38:12639.*
45. Vaughn, D. E., and P. J. Bjorkman. 1997. High affinity binding of the neonatal Fc receptor to its IgG ligand requires receptor immobilization. *Biochemistry 36: 9374.*
46. Stemmer, W. P. 1994. Rapid evolution of a protein in vitro by DNA shuffling. *Nature 370:389.*
47. Deisenhofer, J. 1981. Crystallographic refinement and atomic models of a human Fc fragment and its complex with fragment B of protein A from *Staphylococcus aureus* at 2.9- and 2.8-Å resolution. *Biochemistry 20:2361.*
48. Guex, N., and M. C. Peitsch. 1997. Swiss model and the Swiss-PdbViewer: an environment for comparative protein modeling. *Electrophoresis 18:2714.*